Supplementary Information (SI) for Environmental Science: Advances.

Organogels based on aromatic amino acids with appended long-chain fatty acids for sustainable oil spill recovery and environmental remediation

Abhinandan Bera,[a] Neha Jain,[b] Bikram Das,[c] and Subhasish Roy*[a]

[a] A. Bera, S. Roy, Department of Chemistry, Birla Institute of Technology and Science-Pilani, K K Birla Goa Campus, NH 17B, Zuarinagar, Sancoale, Goa 403726, India, E-mail: subhasishr@goa.bits-pilani.ac.in

[b] N. Jain, Application Specialist, Characterization Division, Anton Paar India Pvt. Ltd., 582, Phase V, Udyog Vihar Industrial Area, Gurgaon – 122016 (Haryana), India.

[c] B. Das, School of Biological Sciences, Indian Association for the Cultivation of Science, 2A & 2B, Raja Subodh Chandra Mallick Rd, Jadavpur, Kolkata-700032, West Bengal, India.

Table of Contents

1. Experimental Section:

1.1 Materials and Methods:

Materials: All the amino acids, L-phenylalanine, L-phenylglycine, and long-chain fatty acids, lauric acid and Palmitic acid, HOBt, disodium hydrogen phosphate, dihydrogen sodium phosphate, sodium carbonate, sodium chloride, all organic solvents used in this work and 100-200 silica mesh were purchased from Sisco Research Laboratories Pvt. Ltd. (SRL) – India. DCC were purchased from Molychem India LLP. Hydrochloric acid was purchased from Avra Synthesis Pvt. Ltd. Ethyl acetate and petroleum ether were purchased from Rankem Laboratory. All chemicals received from the companies were used without further purifications for the synthesis and various experimental studies.

Synthetic Methods and Purifications: Synthesis of these gelator molecules is performed following solution phase peptide synthetic protocol (Scheme S1). Esterification was performed for the C-terminus of the amino acids and then coupled with long-chain fatty acids using HOBt additives in the presence of DCC coupling reagent. The crude compounds were then purified by column chromatography using a 100-200 mesh silica gel with an ethyl acetate and petroleum ether solvent systems.

Preparation of xerogels: Organogels were freeze-dried to obtain xerogels. These xerogels were used for the measurement of X-ray diffraction and FT-IR studies.

1.2 Instrumentation technique and method of analysis:

HR-MS Analysis: All the synthesised compounds masses were confirmed by mass spectrometric analyses by using Q-Tofmicro (Waters Corporation) mass spectrometer.

CHN Analysis: All the synthesised compounds elemental analyses were performed by using Elementar Analysensysteme GmbH, UNICUBE.

Nuclear Magnetic Resonance (NMR) Spectroscopy: All the NMR analyses were done using a Bruker Avance Neo 500 MHz instrument, dissolving in $CDCl_3$ solvent.

X-ray diffraction study: Xerogels obtained from the organogels in different solvents were used to perform powder X-ray diffraction study by using Bruker D8 Advance with Cu-K_α (λ = 0.154 nm).

FT-IR study: IR Affinity-1 (Shimadzu, Japan) was used to measure FT-IR spectra of the xerogels through the attenuated total reflection (ATR) method, where a small amount of xerogels prepared were pressed into contact with the ATR crystal (diamond) to get spectra.

Field emission scanning electron microscopic (FE-SEM) study: To understand morphological behaviour, FE-SEM images were taken in their self-assembled states. 2 µL of organogel was taken from each vial and drop-casted on a glass coverslip and then dried in air and through a vacuum pump. Dilution of the organogels with the corresponding organic solvents followed by 2 µL drop-casting of the self-assembled organogel solutions on a glass coverslip and drying were performed to obtain well separated nanofibrillar morphology. A 3 nm gold coating was performed on the glass coverslip before studying the morphology. FE-SEM images were taken through FEI Quanta FEG 250 scanning electron microscopes by using 10 kV or 20 kV energy.

Rheological Study: Anton Paar, MCR 702e Space Rheometer, was used to find out the mechanical properties and thixotropic behaviour of the organogels. **C_{15}-Phg** and **C_{15}-Phe** organogels in diesel and kerosene at 1.4 % (w/v) and 2.4 % (w/v) concentrations respectively were used for the frequency sweep and thixotropic experiments. Rheometer various parameters details are as follows during the

sample measurements: Fixture type-CP25-1 (cone Plate 25mm diameter with 1degree angle), Diameter- 25 mm, Gap-0.046 mm, Strain magnitude-0.1% and Frequency (0.1-100 rad/s for frequency sweep test) frequency- 0.6283 rad/s or 1Hz and strain 0.1% and 101% for thixotropic test).

Reaction Scheme

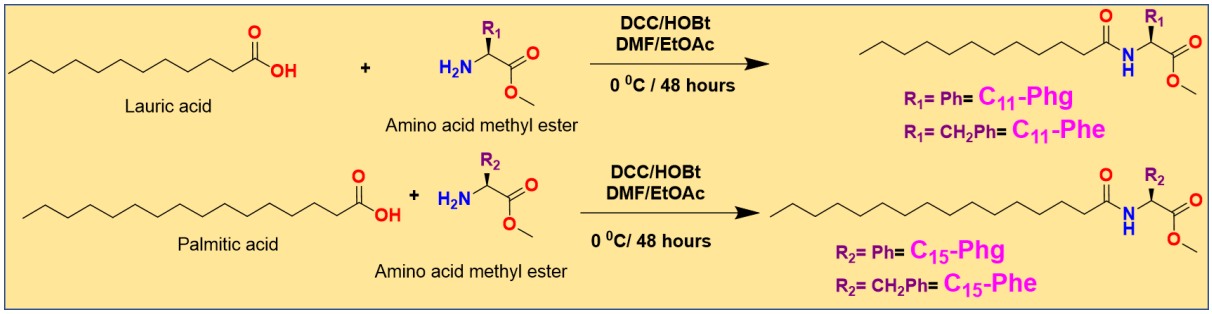

Scheme S1: Synthetic schemes followed for the synthesis of the fatty acids-appended amino acids derivatives (**C_{11}-Phe, C_{11}-Phg, C_{15}-Phe and C_{15}-Phg**).

Synthetic Protocols:

General Synthesis of Acid-Amine Coupling for the syntheses of C_{11}-Phe, C_{11}-Phg, C_{15}-Phe and C_{15}-Phg:

20 millimole of fatty acid (Lauric acid/Palmitic acid) was taken in a dry round-bottom flask. 30 mL of DMF, 20 millimoles of HOBt and methyl ester protected amino acids (L-phenylalanine-OMe / L-phenylglycine-OMe) solution was added followed by stirring the reaction mixture at 0 ^{0}C on an ice bath. 20 millimole of DCC was added to the reaction mixture, and the reaction was stirred for 48 hours. After completion of the reaction, it was filtered to remove DCU. The filtrate was then transferred to a separating funnel and water was added. Aqueous layer was extracted with ethyl acetate (3×30 mL). Then the organic layer was washed with 1(N) HCl solution (3×30 mL), saturated solution of sodium carbonate (3×30 mL), and brine solution (3×30 mL) to remove unreacted reactants and impurities. The organic layer was dried over anhydrous sodium sulphate and then concentrated in a rotavapor to obtain the crude product. The crude material was then purified by column chromatography using a 100-200 mesh silica gel with an ethyl acetate and petroleum ether solvent systems.

Yield of LFM (C_{11}-Phe): 6.85 g white solid (94.87 %)

HR-MS (m/z): Calculated for $C_{22}H_{35}NO_3$: 361.2617, Found: 362.2129 $(M+H)^+$.

Elemental Analysis: Calculated (%) for $C_{22}H_{35}NO_3$: (361.2617): C, 73.09; H, 9.76; N, 3.87; Found C, 74.40; H, 9.926; N, 3.97.

^{1}H NMR (500 MHz, $CDCl_3$, δ in ppm): 0.90 (3H, br), 1.27 (16H, s), 1.60 (2H, br), 2.18 (2H, J=5.69 Hz), 3.11 (1H, dd, J=5.11 Hz, 13.72 Hz), 3.18 (1H, dd, J=5.29 Hz, 14.29 Hz), 3.75 (3H, s), 4.92-4.93 (1H, br, m), 5.88 (1H, d, J=5.69 Hz), 7.11 (2H, d, J=6.37 Hz), 7.28-7.30 (3H, br, m).

^{13}C NMR (126 MHz, $CDCl_3$, δ in ppm): 172.77, 172.21, 135.89, 129.27, 128.57, 127.13, 52.91, 52.35, 37.91, 36.57, 31.93, 29.63, 29.49, 29.36, 29.22, 25.59, 22.71, 14.15.

DEPT 135 (126 MHz, $CDCl_3$, δ in ppm): 129.77, 128.57, 127.13, 52.91, 52.34, 37.91, 36.57, 31.93, 29.63, 29.49, 29.36, 29.22, 25.58, 22.71, 14.15.

Yield of LPM (C_{11}-Phg): 4.9 g white solid (70.60 %)

HR-MS (m/z): Calculated for $C_{21}H_{33}NO_3$: 347.2460, Found: 348.1945 $(M+H)^+$.

Elemental Analysis: Calculated (%) for $C_{21}H_{33}NO_3$: (347.2460): C, 72.58; H, 9.57; N, 4.03; Found C, 73.88; H, 9.747; N, 4.11.

^{1}H NMR (500 MHz, $CDCl_3$, δ in ppm): 0.90 (3H, t, J=6.99 Hz), 1.27-1.30 (16H, br), 1.65 (2H, br, m), 2.26 (2H, br, m), 3.75 (3H, s), 5.62 (1H, d, J=6.95 Hz), 6.44 (1H, d, J=5.20 Hz), 7.37 (5H, br, m).

^{13}C NMR (126 MHz, $CDCl_3$, δ in ppm): 172.53, 171.59, 136.64, 128.99, 128.54, 127.28, 56.28, 52.82, 36.41, 31.95. 29.72, 29.68, 29.62, 29.49, 29.39, 29.35, 29.23, 25.51, 22.72, 14.16.

DEPT 135 (126 MHz, $CDCl_3$, δ in ppm): 128.99, 128.54, 127.27, 56.28, 52.82, 36.41, 31.95, 29.71, 29.68, 29.62, 29.49, 29.39, 29.34, 29.22, 25.51, 22.72, 14.16.

Yield of PFM (C_{15}-Phe): 7.22 g white solid (86.47 %)

HR-MS (m/z): Calculated for $C_{26}H_{43}NO_3$: 417.3243, Found: 418.2601 $(M+H)^+$.

Elemental Analysis: Calculated (%) for $C_{26}H_{43}NO_3$: (417.3243): C, 74.78; H, 10.38; N, 3.35; Found C, 76.30; H, 10.464; N, 3.46.

^{1}H NMR (500 MHz, $CDCl_3$, δ in ppm): 0.90 (3H, br), 1.27 (24H, s), 1.60 (2H, br, m), 2.18 (2H, t, J=6.97 Hz), 3.11 (1H, dd, J=5.33 Hz, 13.66 Hz), 3.18 (1H, dd, J=5.51 Hz, 13.76 Hz), 3.75 (3H, s), 4.92 (1H, br, m), 5.88 (1H, d, J=6.38 Hz), 7.11 (2H, d, J=6.77 Hz), 7.26-7.30 (3H, br, m).

^{13}C NMR (126 MHz, $CDCl_3$, δ in ppm): 172.72, 172.21, 135.90, 129.27, 128.56, 127.12, 52.90, 52.32, 37.93, 36.58, 31.94, 29.71, 29.67, 29.63, 29.49, 29.38, 29.35, 29.22, 25.57, 22.71, 14.14.

DEPT 135 (126 MHz, $CDCl_3$, δ in ppm): 129.27, 128.56, 127.12, 52.90, 52.32, 37.92, 36.58, 31.94, 29.70, 29.68, 29.64, 29.49, 29.37, 29.35, 29.22, 25.57, 22.71, 14.14.

Yield of PPM (C_{15}-Phg): 7.34 g white solid (91.18 %)

HR-MS (m/z): Calculated for $C_{25}H_{41}NO_3$: 403.3086, Found: 404.2470 $(M+H)^+$.

Elemental Analysis: Calculated (%) for $C_{25}H_{41}NO_3$: (403.3086): C, 74.40; H, 10.24; N, 3.47; Found C, 75.99; H, 10.357; N, 3.51.

^{1}H NMR (500 MHz, $CDCl_3$, δ in ppm): 0.89 (3H, t, J=6.72 Hz), 1.27 (24H, s), 1.64 (2H, br, m), 2.25 (2H, br, m), 3.74 (3H, s), 5.61 (1H, d, J=6.94 Hz), 6.48 (1H, d, J=5.75 Hz), 7.37 (5H, br).

^{13}C NMR (126 MHz, $CDCl_3$, δ in ppm): 172.53, 171.59, 136.64, 128.99, 128.54, 127.28, 56.28, 52.82, 36.41, 31.95, 29.72, 29.68, 29.62, 29.49, 29.39, 29.35, 29.23, 25.51, 22.71, 14.16.

DEPT 135 (126 MHz, $CDCl_3$, δ in ppm): 128.99, 128.54, 127.27, 56.28, 52.82, 36.41, 31.95, 29.71, 29.68, 29.62, 29.49, 29.39, 29.34, 29.22, 25.51, 22.72, 14.16.

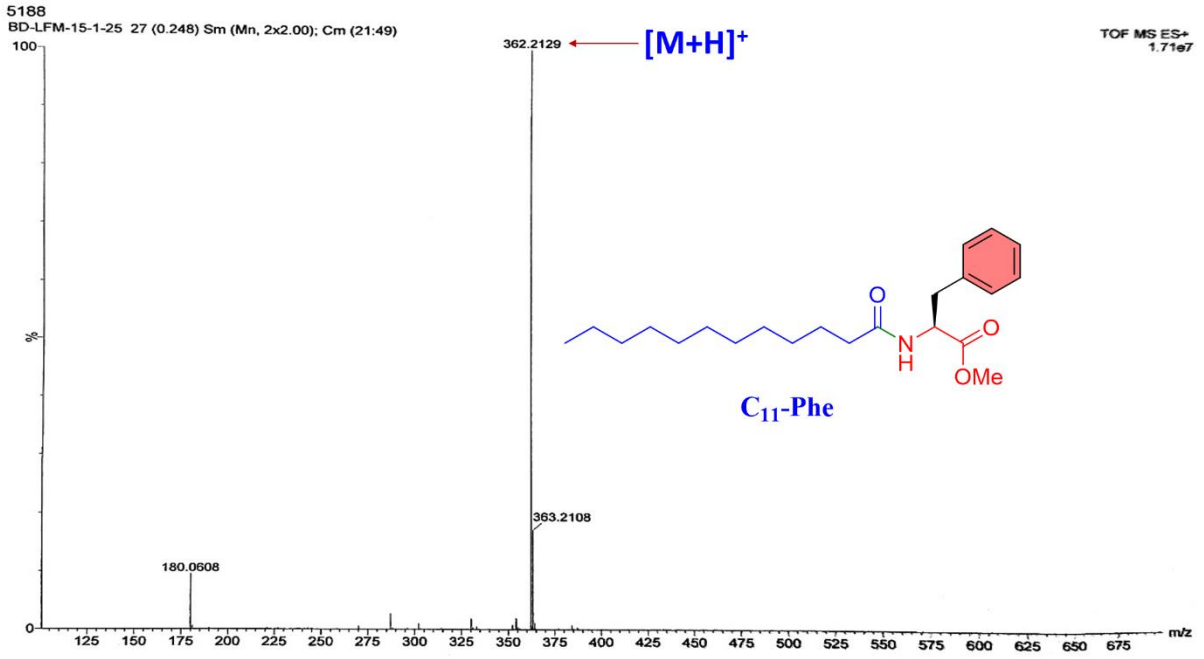

Fig. S1: HR-MS spectrum of **C_{11}-Phe** (**LFM**) in positive mode.

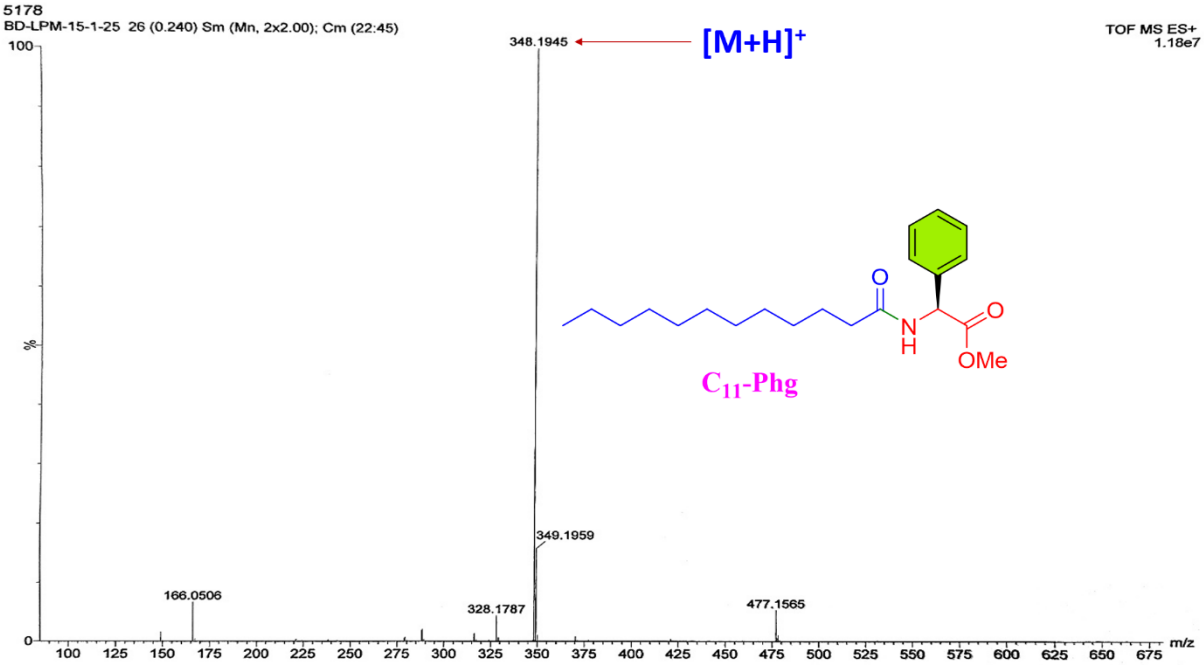

Fig. S2: HR-MS spectrum of **C_{11}-Phg** in positive mode.

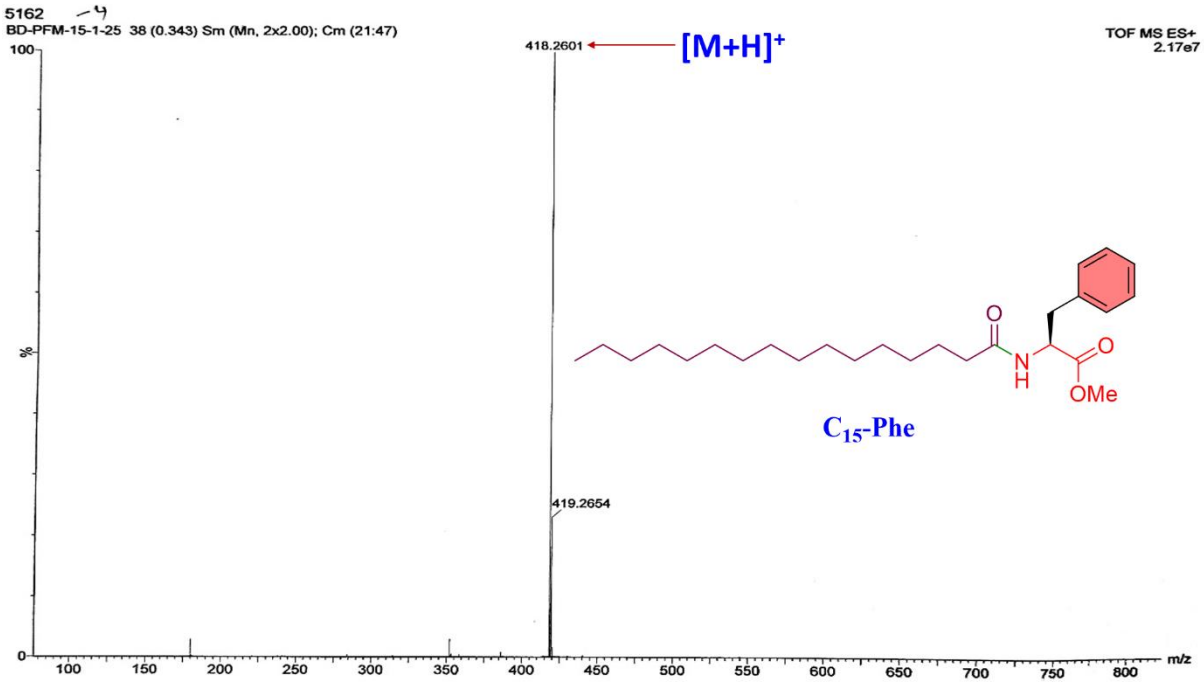

Fig. S3: HR-MS spectrum of **C_{15}-Phe** in positive mode.

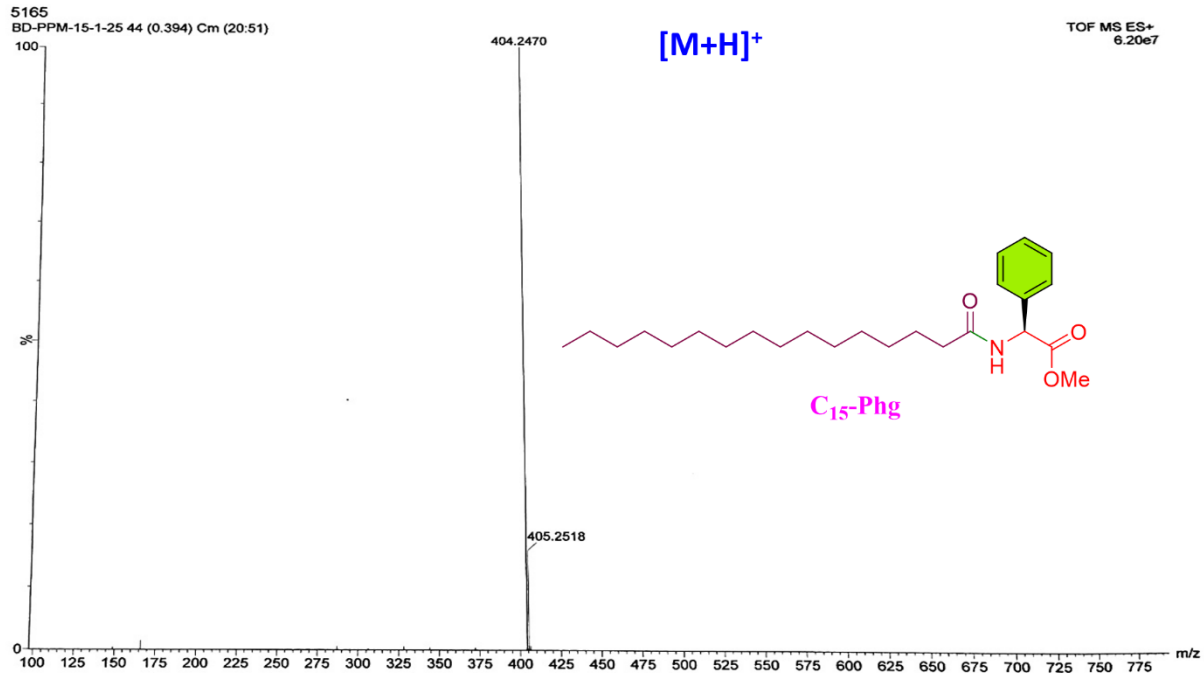

Fig. S4: HR-MS spectrum of **C_{15}-Phg** in positive mode.

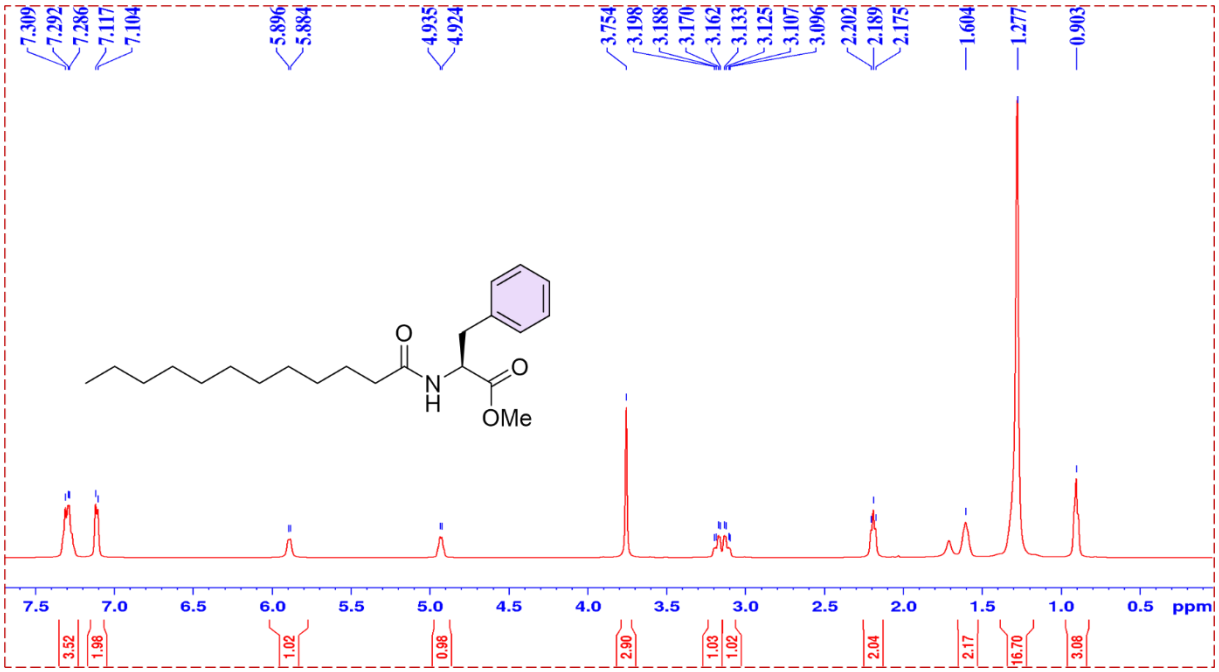

Fig. S5: ^{1}H NMR spectrum of **C_{11}-Phe** in $CDCl_3$.

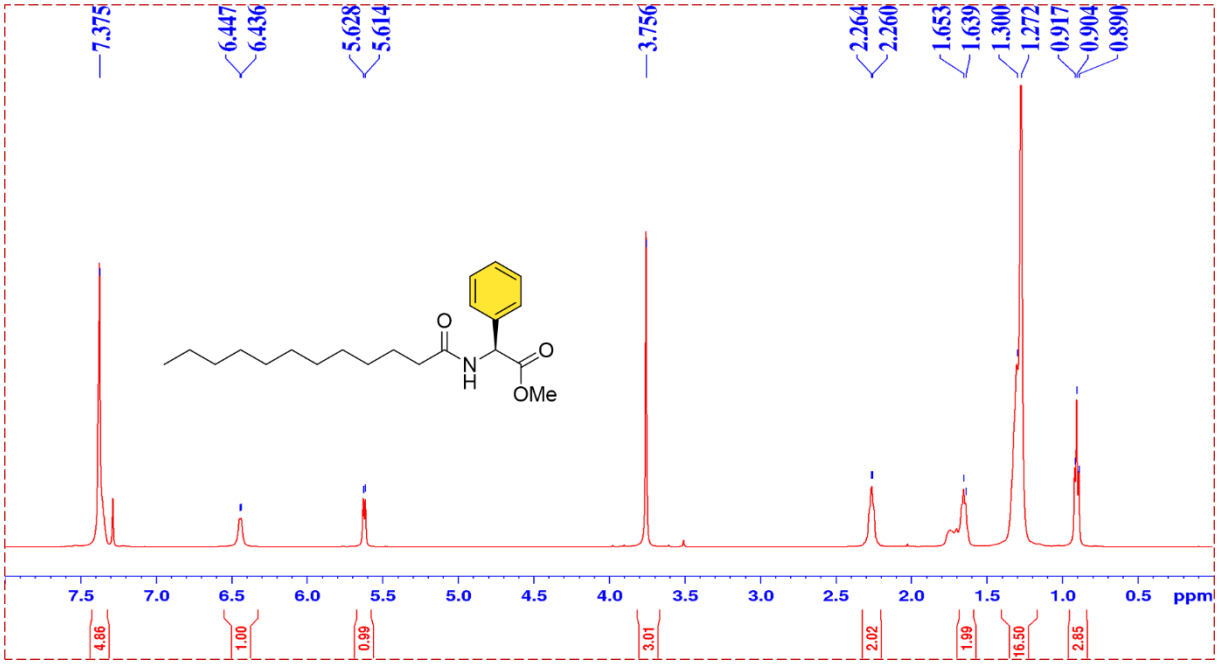

Fig. S6: ^{1}H NMR spectrum of **C_{11}-Phg** in $CDCl_3$.

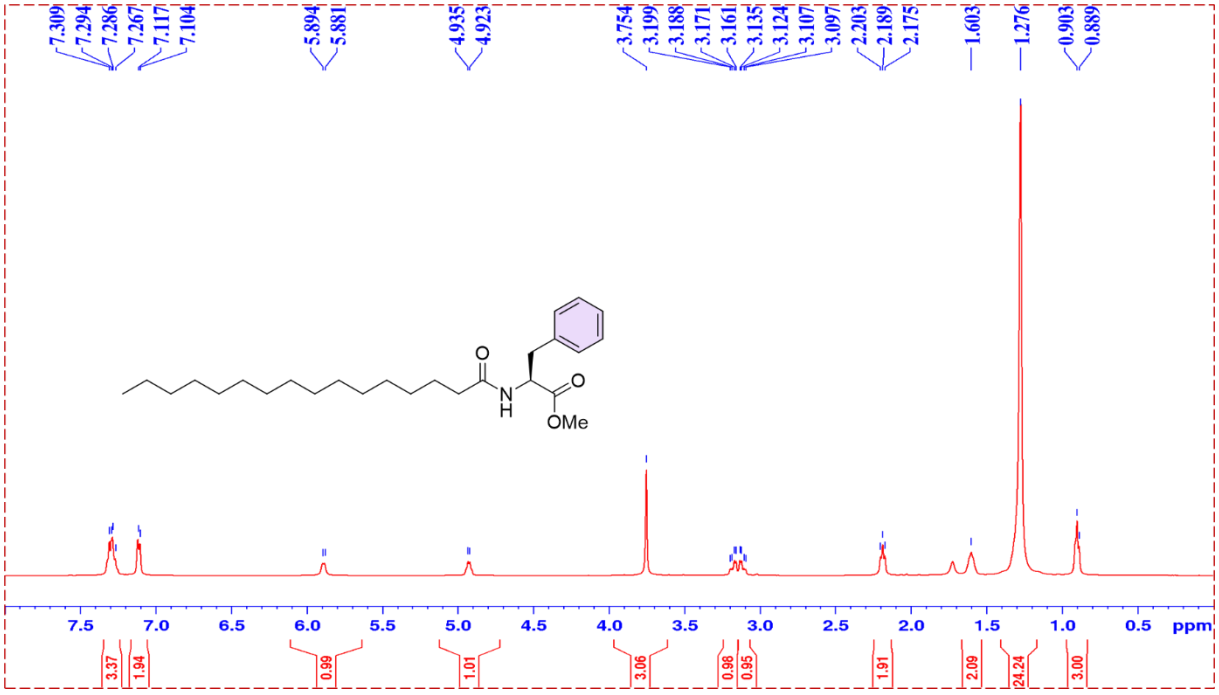

Fig. S7: ^{1}H NMR spectrum of **C_{15}-Phe** in $CDCl_3$.

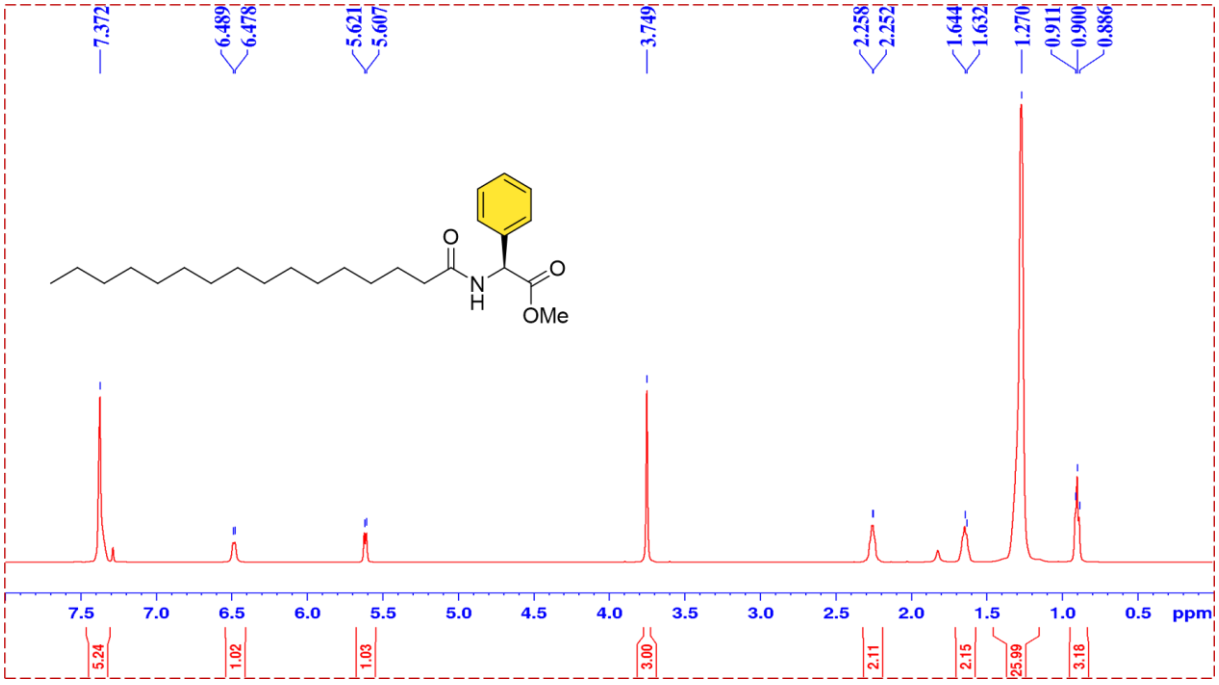

Fig. S8: ^{1}H NMR spectrum of **C_{15}-Phg** in $CDCl_3$.

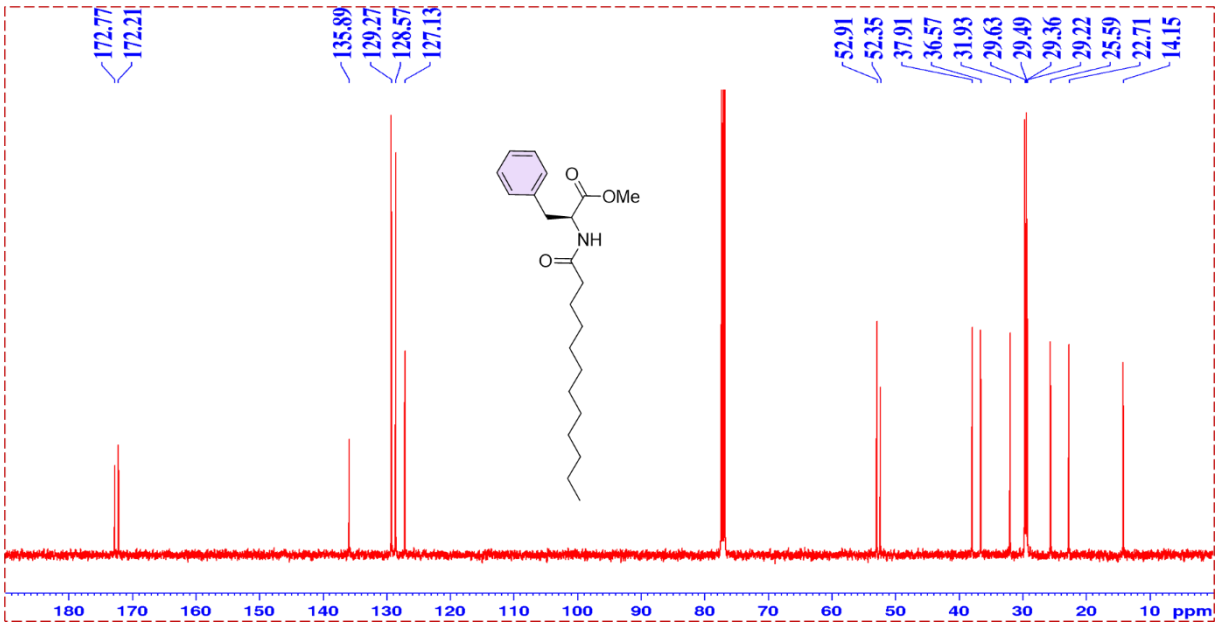

Fig. S9: ^{13}C NMR spectrum of **C_{11}-Phe** in $CDCl_3$.

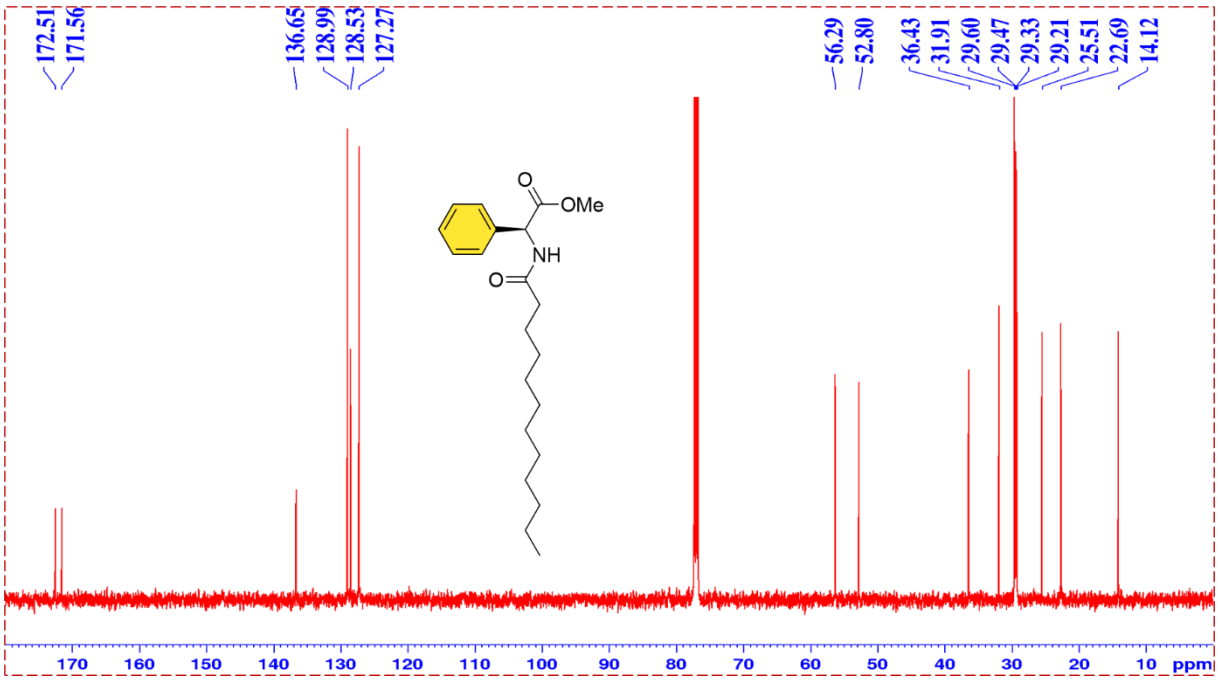

Fig. S10: ^{13}C NMR spectrum of **C_{11}-Phg** in $CDCl_3$.

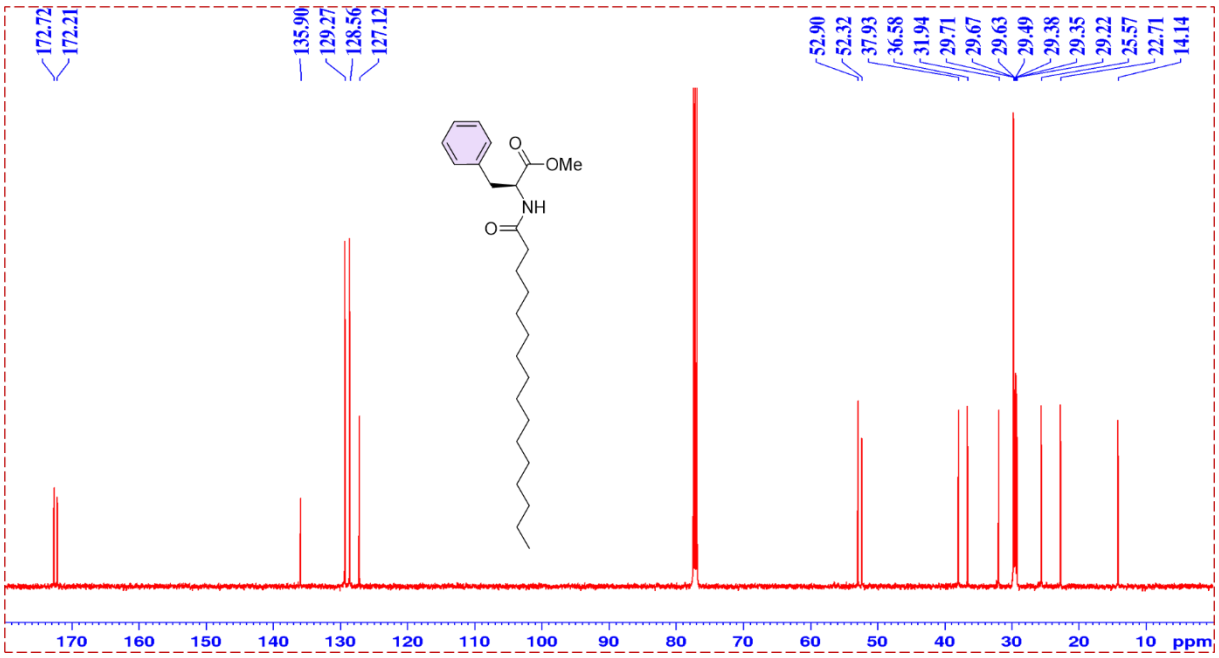

Fig. S11: ^{13}C NMR spectrum of **C_{15}-Phe** in $CDCl_3$.

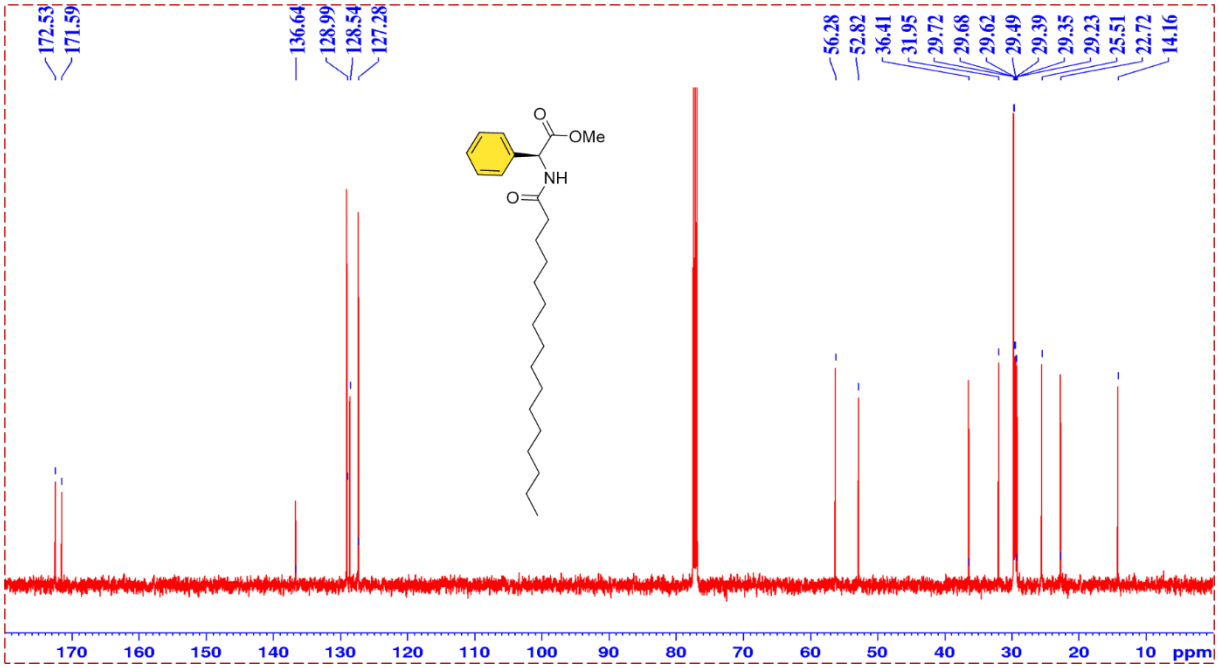

Fig. S12: ^{13}C NMR spectrum of **C_{15}-Phg** in $CDCl_3$.

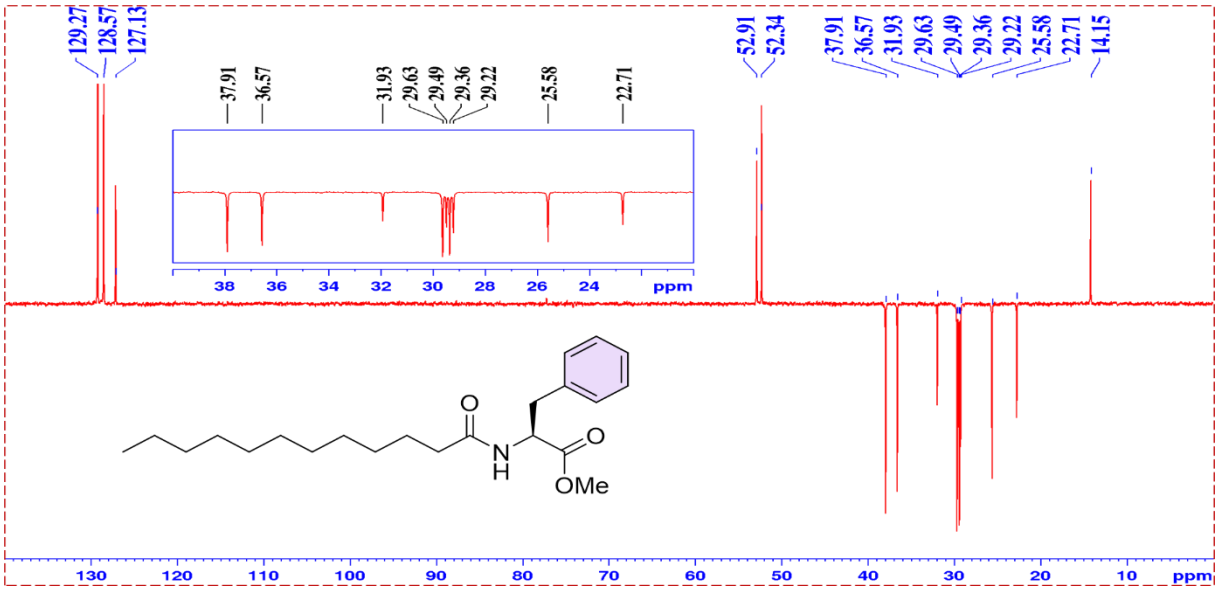

Fig. S13: DEPT 135 spectrum of **C_{11}-Phe** in $CDCl_3$.

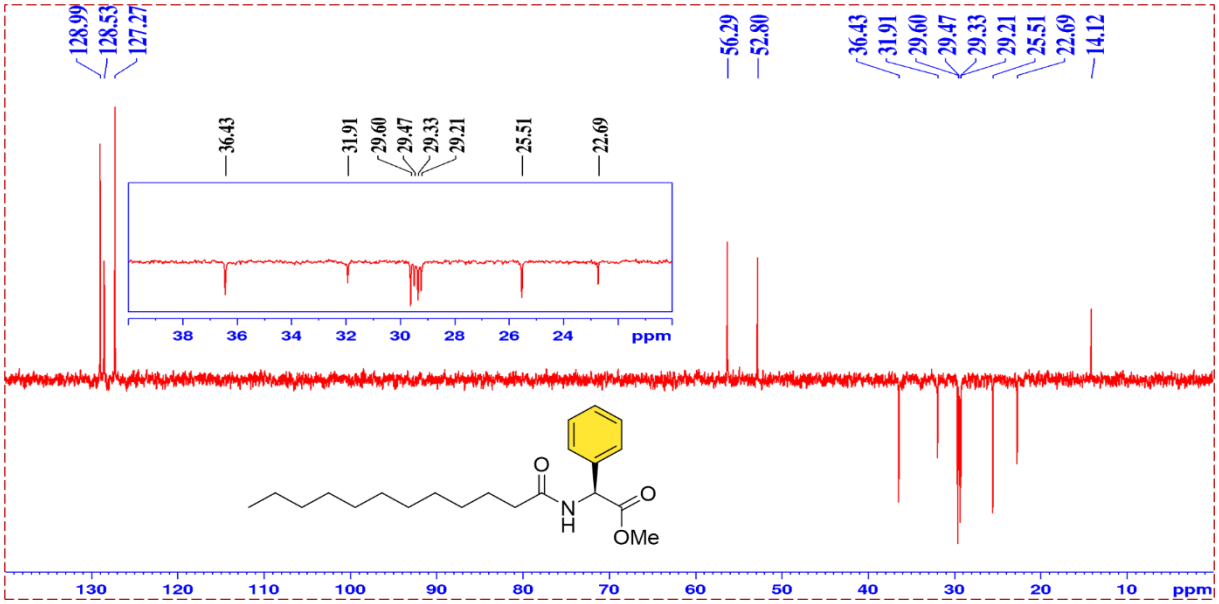

Fig. S14: DEPT 135 spectrum of **C_{11}-Phg** in $CDCl_3$.

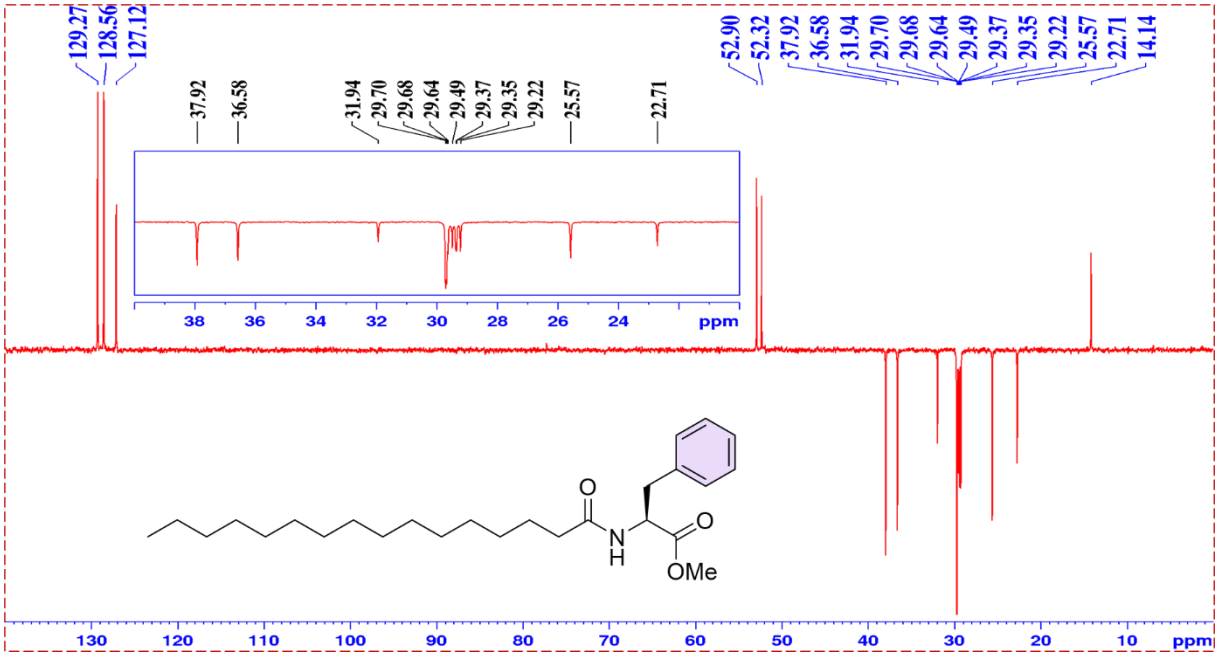

Fig. S15: DEPT 135 spectrum of **C_{15}-Phe** in $CDCl_3$.

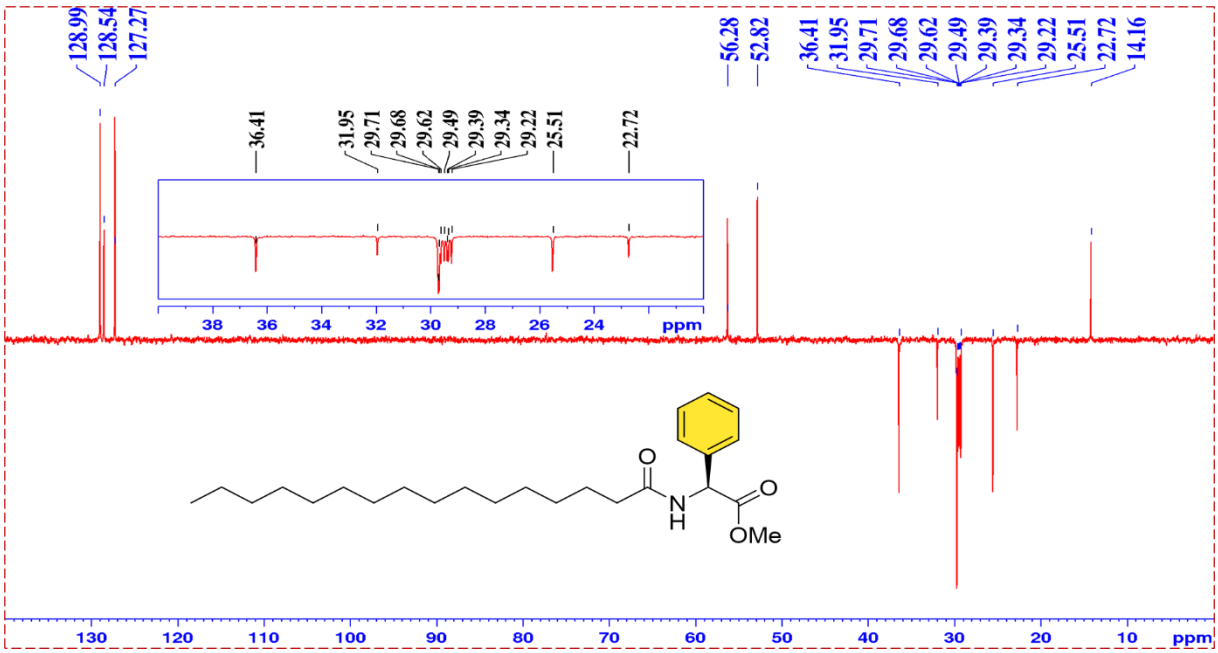

Fig. S16: DEPT 135 spectrum of **C_{15}-Phg** in $CDCl_3$.

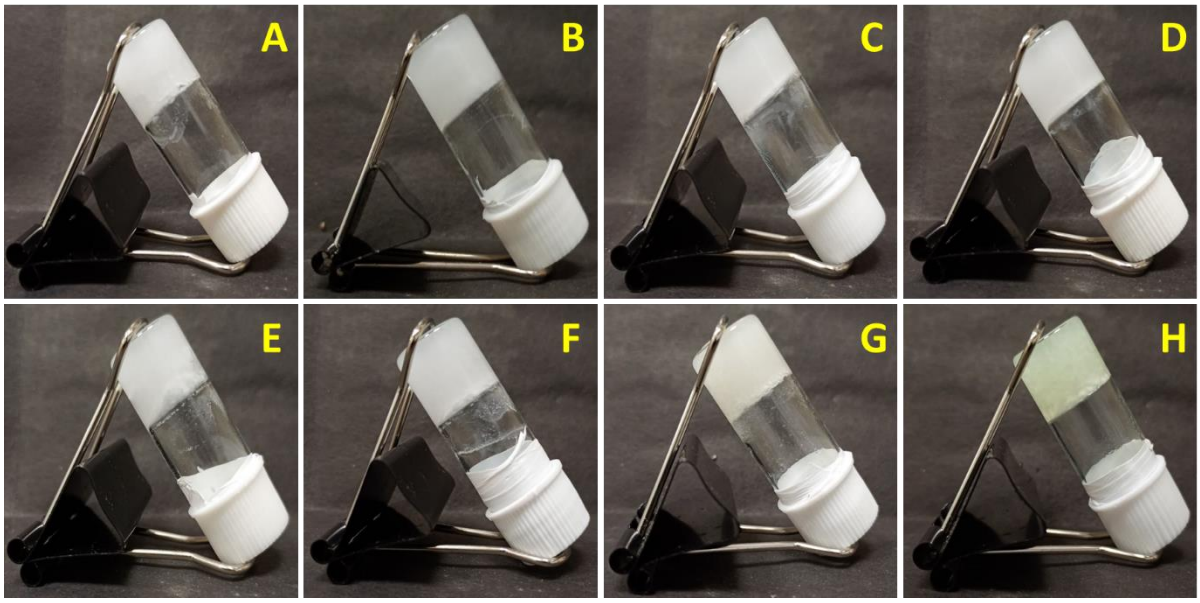

Fig. S17: Organogels of **C_{15}-Phe** in isooctane (**A**), heptane (**B**), cyclohexane (**C**), methyl cyclohexane (**D**), hexane (**E**), petroleum ether (**F**), kerosene (**G**) and diesel (**H**).

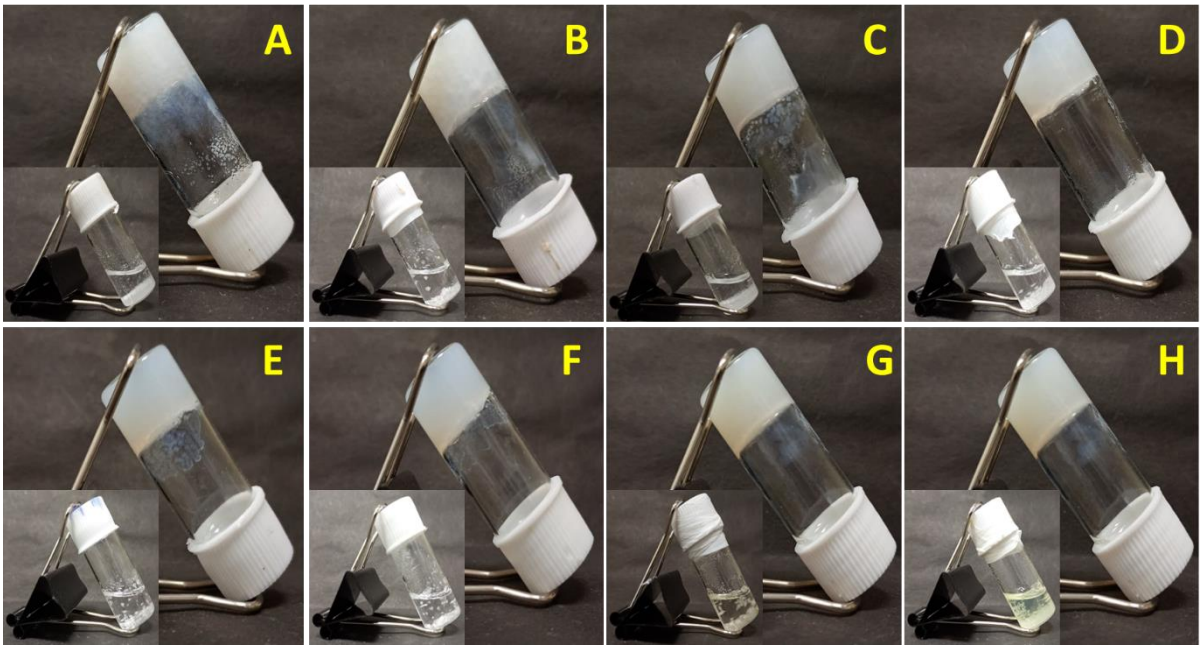

Fig. S18: Organogels of **C_{11}-Phg** in isooctane (**A**), heptane (**B**), cyclohexane (**C**), methyl cyclohexane (**D**), hexane (**E**), petroleum ether (**F**), kerosene (**G**) and diesel (**H**) in their gel states and after precipitations with time.

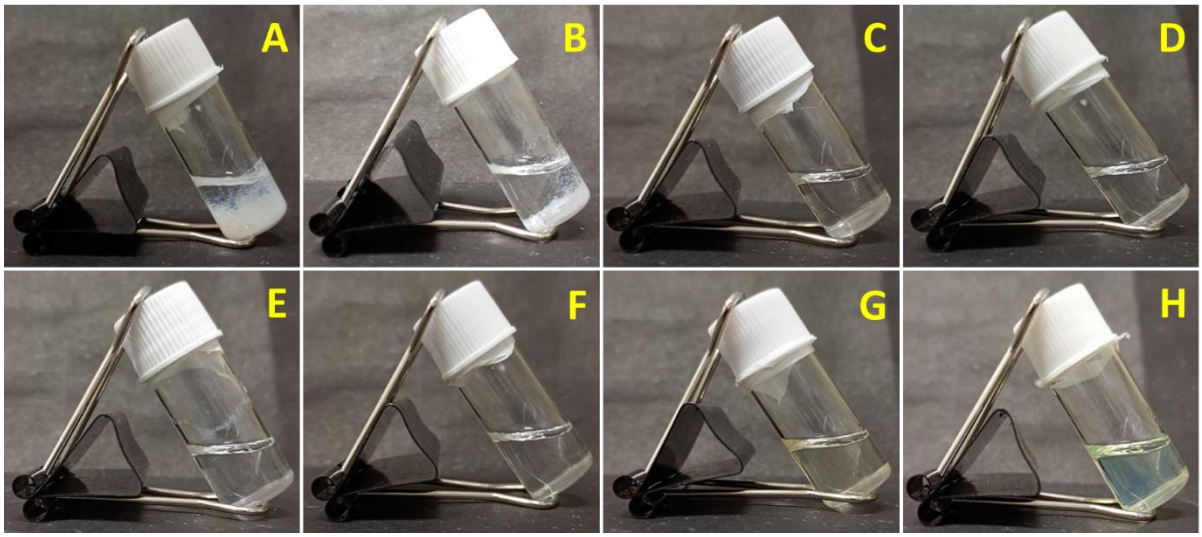

Fig. 19: Precipitations of **C_{11}-Phe** in isooctane (**A**) and in n-heptane (**B**) solvent. Transparent solution formations in cyclohexane (**C**), methyl cyclohexane (**D**), hexane (**E**), petroleum ether (**F**), kerosene (**G**) and diesel (**H**).

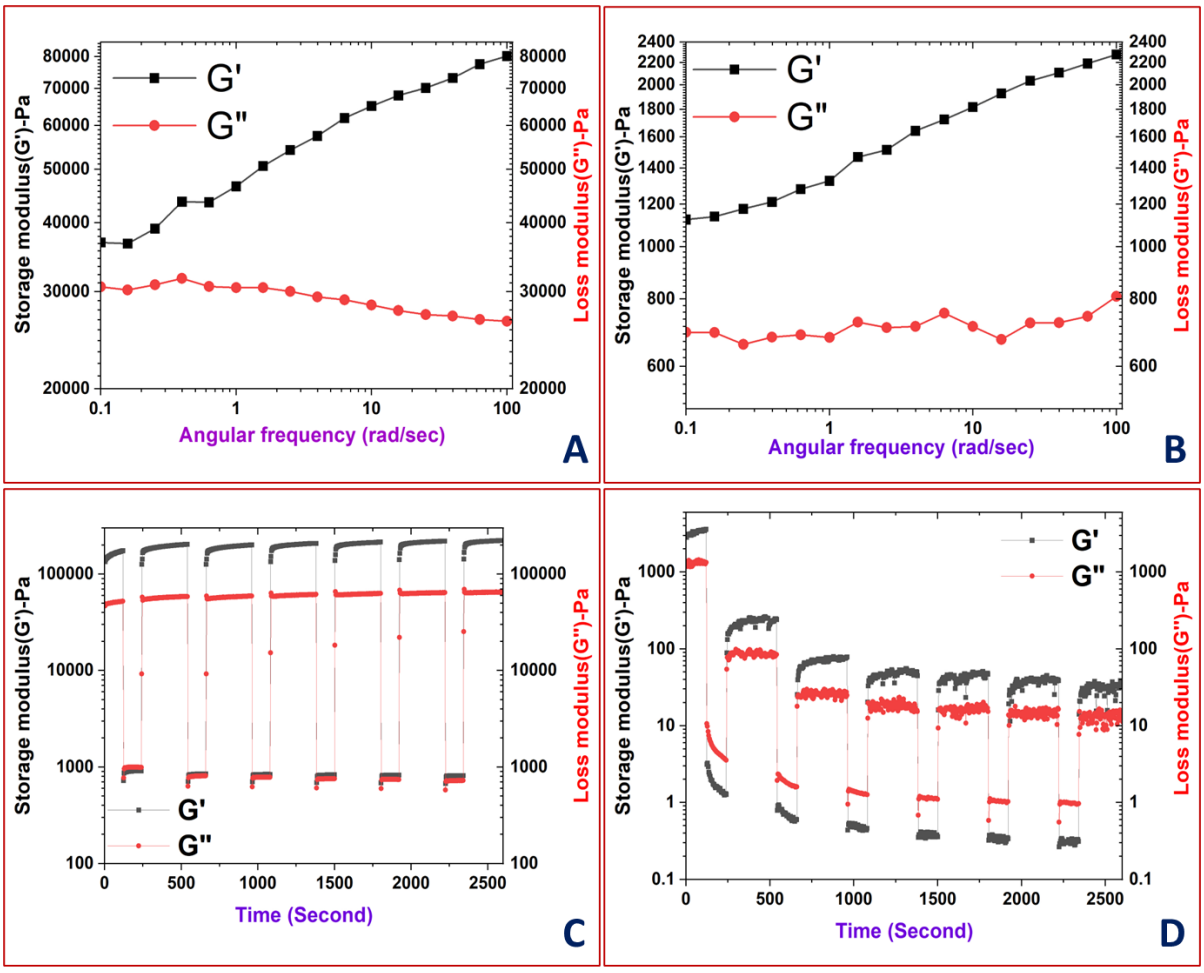

Fig. S20: Frequency sweep profile of **C_{15}-Phe** gel in kerosene (**A**) and in diesel (**B**). Thixotropic step-strain profile of **C_{15}-Phe** gel in kerosene (**C**) and in diesel (**D**).

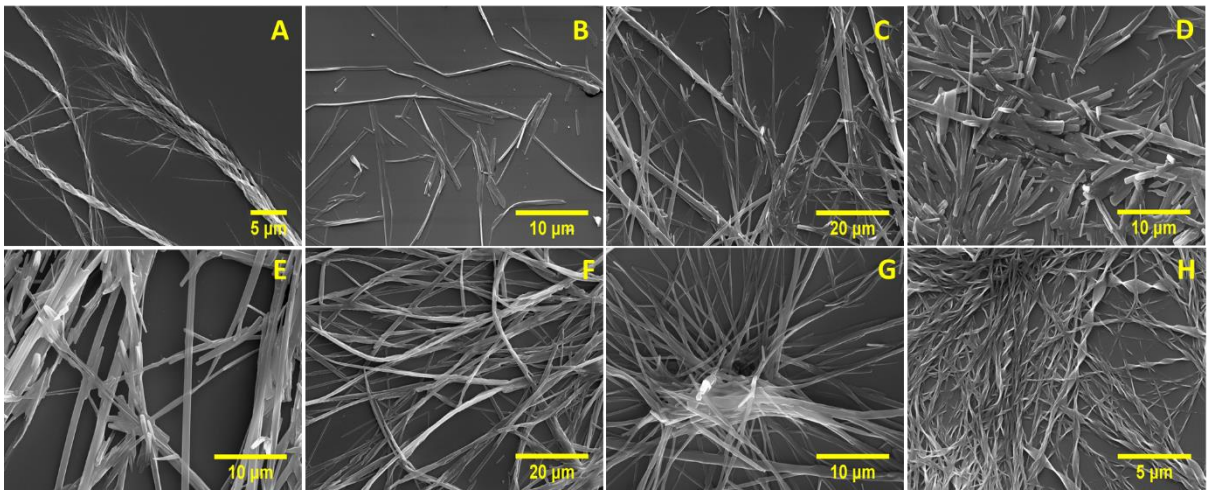

Fig. S21: FE-SEM images of **C_{15}-Phe** gelator in isooctane (**A**), heptane (**B**), cyclohexane (**C**), methyl cyclohexane (**D**), hexane (**E**), petroleum ether (**F**) and kerosene (**G**) solvents. **H** represent the FE-SEM image of **C_{11}-Phg** gel in isooctane solvent.

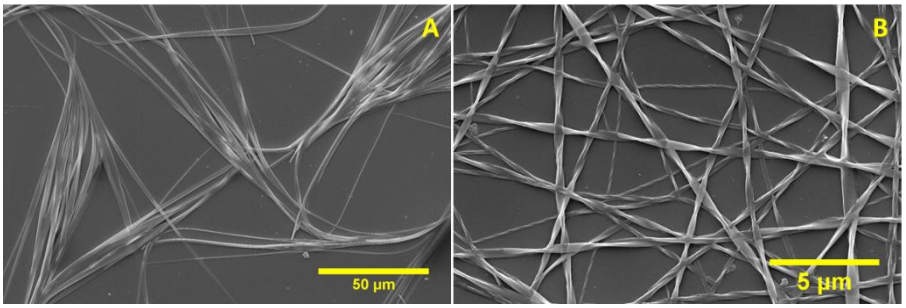

Fig. S22: FE-SEM images of **C_{11}-Phe** (**A**) and **C_{11}-Phg** (**B**) in kerosene.

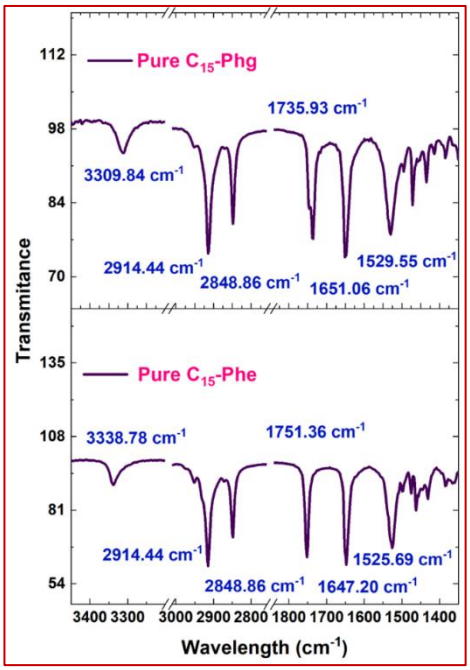

Fig. S23: FT-IR spectrum of pure solid **C_{15}-Phg** and **C_{15}-Phe** gelator molecules.

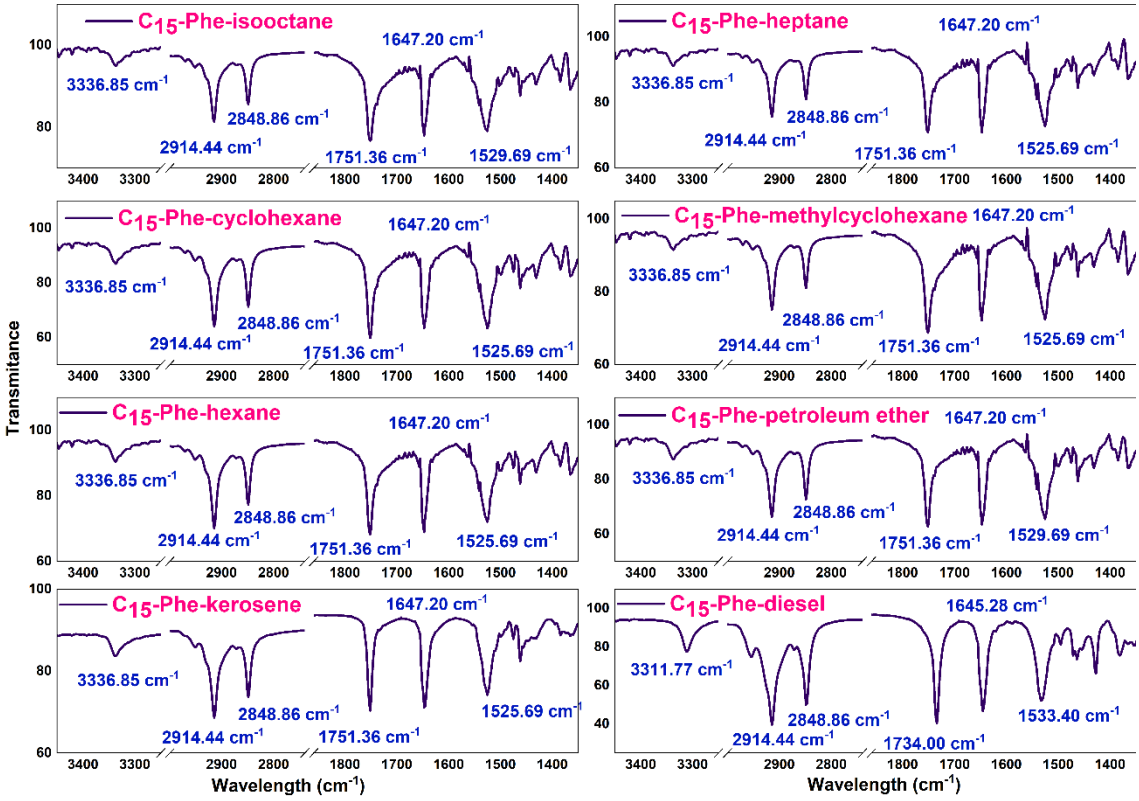

Fig. S24: FT-IR spectra of xerogels of **C_{15}-Phe** gelator in isooctane, heptane, cyclohexane, methyl cyclohexane, hexane, petroleum ether and kerosene solvents.

Table S1: FT-IR stretching frequencies of pure solid compound and xerogels of **C_{15}-Phg** gelator in different solvents.

C_{15}-Phg	N-H stretching frequency (cm^{-1})	Alkane stretching frequency (cm^{-1})	C=O stretching frequency of ester (cm^{-1})	C=O stretching frequency of amide (cm^{-1})	N-H bending frequency of amide (cm^{-1})
Pure Solid	3309.84	2914.44, 2848.86	1735.93	1651.06	1529.55
Isooctane-xerogel	3315.63	2914.44, 2848.86	1735.93	1651.06	1531.47
Heptane-xerogel	3315.63	2914.44, 2848.86	1735.93	1649.13	1529.55
Cyclohexane-xerogel	3309.84	2914.44, 2848.86	1735.93	1645.28	1535.33
Methylcyclohexane-xerogel	3313.70	2914.44, 2848.86	1737.86	1649.13	1529.55
Hexane-xerogel	3313.70	2914.44, 2848.86	1735.93	1649.13	1529.55
Petroleum ether-xerogel	3313.70	2914.44, 2848.86	1735.93	1649.13	1531.47
Kerosene-xerogel	3315.63	2914.44, 2848.86	1735.93	1649.13	1531.47
Diesel-xerogel	3315.63	2914.44, 2848.86	1751.36	1647.20	1525.69

Table S2: FT-IR stretching frequencies of pure solid compound and xerogels of **C_{15}-Phe** gelator of different solvents in tabular form.

C_{15}-Phe	N-H stretching frequency (cm^{-1})	Alkane stretching frequency (cm^{-1})	C=O stretching frequency of ester (cm^{-1})	C=O stretching frequency of amide (cm^{-1})	N-H bending frequency of amide (cm^{-1})
Pure Solid	3338.78	2914.44, 2848.86	1751.36	1647.20	1529.69
Isooctane-xerogel	3336.85	2914.44, 2848.86	1751.36	1647.20	1529.69
Heptane-xerogel	3336.85	2914.44, 2848.86	1751.36	1647.20	1525.69
Cyclohexane-xerogel	3336.85	2914.44, 2848.86	1751.36	1647.20	1525.69
Methylcyclohexane-xerogel	3336.85	2914.44, 2848.86	1751.36	1647.20	1525.69
Hexane-xerogel	3336.85	2914.44, 2848.86	1751.36	1647.20	1525.69
Petroleum ether-xerogel	3336.85	2914.44, 2848.86	1751.36	1647.20	1529.69
Kerosene-xerogel	3336.85	2914.44, 2848.86	1751.36	1647.20	1525.69
Diesel-xerogel	3311.77	2914.44, 2848.86	1734.00	1645.28	1533.40

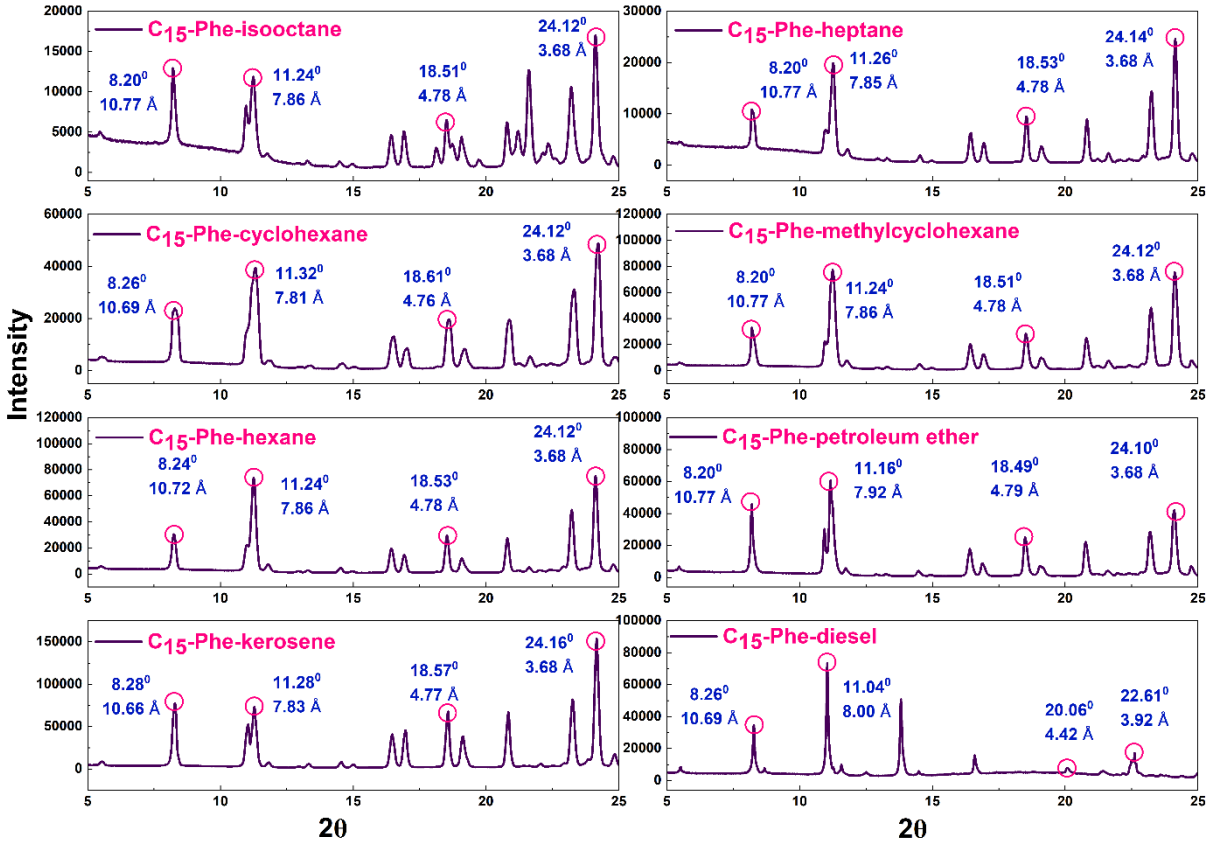

Fig. S25: FT-IR spectrum of xerogels of **C_{15}-Phe** gelator in isooctane, heptane, cyclohexane, methyl cyclohexane, hexane, petroleum ether and kerosene solvents.